

Peak Luminosities of Bursts from GRO J1744-28 measured with the RXTE PCA;

Italia: wij post 17 two 4s - a one man marching band - got darn bright.

Keith Jahoda, Michael J. Stark, Tod E. Strohmayer, William Zhang, ^a Edward H. Morgan, and Derek Fox ^b

^aLaboratory for High Energy Astrophysics, Goddard Space Flight Center, Code 662, Greenbelt, MD, 20771 USA

^bCenter for Space Research, MIT, Cambridge, MA, 02138

GRO J1744-28, discovered by BATSE in December 95, is the second neutron star system known to produce frequent accretion powered bursts. The system has been regularly monitored with the RXTE PCA since the peak of the first outburst in January 96 at which time the observed persistent and bursting count rates were $\sim 25,000$ ct/sec and $\sim 150,000$ ct/sec, with corresponding instrumental deadtimes of $\sim 10\%$ and $\geq 50\%$. We present a model which allows the reconstruction of the true incident count rate in the presence of enormous deadtime and use the model to derive a history of the peak luminosities and fluences of the bursts as a function of time. During the peak of the January 1996 and January 1997 outbursts, when the persistent emission was ≥ 1 Crab, we infer peak luminosities of ~ 100 times the Eddington luminosity, and a ratio of persistent emission to integrated burst emission of ~ 34 .

1. GRO J1744-28

GRO J1744-28, the “bursting pulsar” was discovered by the Burst And Transient Source Experiment (BATSE) in December 1995 [1] just prior to the launch of the Rossi X-ray Timing Explorer (RXTE) on 30 December 1995. RXTE has performed a series of observations of this object from January 1996 through November 1997 during which time the source has varied from having a persistent flux in excess of 1 Crab with bursts which saturated the Proportional Counter Array (PCA) to being undetectable. The PCA observations complement the nearly continuous BATSE record by virtue of the large collecting area and high time resolution of the PCA and High Energy X-ray Timing Experiment (HEXTE) experiments. These pointed experiments can study individual bursts in much greater detail and follow the evolution of the outbursts to much fainter fluxes than BATSE. Studies of the individual bursts has, until now, been handicapped by an incomplete understanding of the deadtime processes in the PCA when observing extremely

bright sources. The three main purposes of this contribution are to (a) present a model of deadtime processes in the PCA which is reliable for input fluxes at least up to 35 Crab ($\sim 0.5 \times 10^6$ count/sec); (b) establish that the bursts from J1744-28 reached luminosities of ~ 100 times the Eddington luminosity; and (c) to provide advice to users of RXTE who may observe sources brighter than 5 Crab during the rest of the RXTE mission.

2. EVIDENCE OF SATURATION

Figure 1 shows, for one burst observed on 1996 February 4 and which peaked at 13:15:33 UTC, the observed good event rate as well as the *Remaining Counts* rate from the Standard 1 data plotted with 0.125 second time bins. The Standard 1 data (present for all PCA observations) contains 8 rates, read out every 0.125 seconds and internal calibration spectra. The eight rates consist of the good rate in each of the 5 detectors, the sum over 5 detectors of all events which trigger only the propane layer, all events which

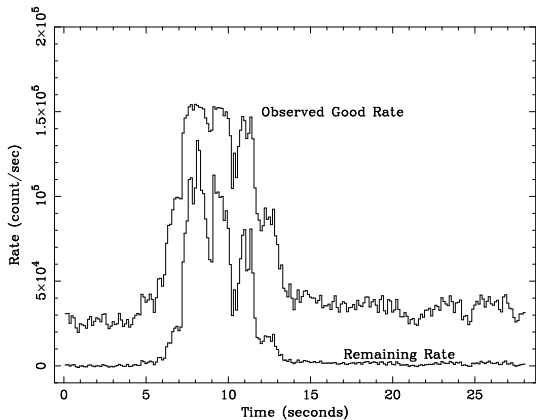


Figure 1. Good and Coincidence rates observed from a 1996 February 4 burst.

trigger the VLE flag (i.e. saturating events), and all other events commonly called the *Remaining Counts* rate. For most observations, the remaining Counts rate is dominated by particle induced background events; for bright sources there is a non trivial possibility that two (or more) cosmic X-rays will be detected in different parts of the detector and be recorded as a multiple anode event. The sudden rise in the Remaining Counts rate, coincident in time with the rise in the Good event rate, makes it clear that in the burst, the remaining counts rate is dominated by the coincidences of photons which arise in the burst.

It is however obvious that while the good event rate reaches an apparent plateau around 1.5×10^5 count/sec, the remaining count rate has a structure with greater contrast. This observation suggests the central theme of our deadtime correction: the rate of coincident events, which depends on the square of the incident rate, is a better measure of the flux of very bright sources than the good rate. Information on the coincidence rate is always available on 0.125 second scales, and can be available with higher time resolution through the use of EDS modes which count and telemeter events which trigger exactly two anode chains. (For a complete list of modes see [2].)

Examination of numerous bursts from January

and February 1996 show similar characteristics: the good rate saturates near 1.5×10^5 count/sec while the remaining rate shows much larger relative variations.

3. PCA AND EDS CHARACTERISTICS

3.1. PCA

Each Proportional Counter Unit (PCU) has 9 independent signal chains. Seven signal chains, designated L1, R1, L2, R2, L3, R3, and VP, signifying the “left” and “right” halves of the three Xenon layers and the propane veto layer [3] have individual charge sensitive pre-amplifiers and shaping amplifiers and share a common analog to digital converter (ADC). The xenon veto anodes and the calibration flag set discriminators but are not pulse height analyzed. A good event is one which triggers exactly one signal chain; the pulse height from the ADC is unambiguously associated with that signal chain. An event which triggers two or more chains produces two flags and a pulse height which could correspond to either chain (but in any case which contains only a fraction of the deposited energy) and is generally discarded as a non X-ray event. (An event which triggers the calibration flag and one other anode chain is an exception to this rule and is tagged as a calibration event.) The analog pulse shaping is a paralyzable process while the analog to digital conversion is a non-paralyzable process.

3.2. EDS

The EDS always runs two Standard modes in addition to the data modes selected by the observer. A key feature of each of these modes is that every PCA event is recorded exactly once. Standard 1 produces 8 rates read out every 0.125 seconds while Standard 2 produces a spectrum for each signal chain and 29 distinct coincidence rates for each PCU once every 16 seconds. In special circumstances, the Standard 2 mode can be read out on shorter time scales. We present, in the next section, data obtained while observing bright sources with the Standard 2 mode being read out more frequently than usual. These data allow us to parameterize a model of PCA dead-time processes.

4. DEADTIME MODEL

Here we present data obtained while slowly scanning over Sco X-1 (with a 1 second readout interval for the Standard 2 data) and data obtained during a bright burst from J1744-28 (with 2 second readout). The details of the paralyzable deadtime process associated with the analog pulse shaping are pulse height dependent, so we expect some differences in parameters derived from Sco X-1 (a very soft source) and J1744-28 (a very hard source).

Figure 2 shows two rates observed during a scan over Sco X-1 (97Mar15). The smooth curve represents the collimator efficiency for one of the PCU, and the histograms represent the counting rate observed in the L1 layer (i.e. good events) and the rate of L1 plus R1 coincidences (two photons observed within the coincidence window, one on each half of the first layer). The collimator efficiency is scaled to demonstrate that the L1 rate is affected by a 25 – 30% deadtime near the peak of the collimator transmission. We believe that we can treat Sco X-1 as a constant source for these purposes; the presence of a nearly stationary 6 Hz QPO at the time of these observations indicates that Sco X-1 was in the normal branch with a momentarily stable mass accretion and luminosity.

Figure 3 shows the same rate data, plotted against each other. The rate data have been corrected for the non paralyzable deadtime associated with the analog to digital conversion (and which must account for all events in this detector, not just the two rates that are plotted). Also shown is the best fit which models the L1+R1 rate as a constant plus a term proportional to the square of the L1 rate. The fit considers only points with a corrected L1 rate $\leq 10^4$ count/sec, although the figure shows the fit extrapolated to the highest observed rates. The constant represents a background term, while the quadratic coefficient represents the average time window during which a coincidence can be recorded. The average is over pulse height as we have ignored all energy information while creating this correlation. Identifying the L1 and R1 rates as the same (due to their identical construction), we ex-

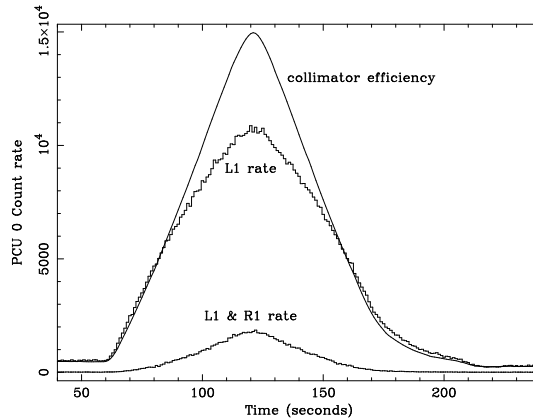


Figure 2. Collimator transmission, L1 rate, and L1+R1 rate for one PCU during scan over Sco X-1 in normal branch

pect that the quadratic term represents twice the coincidence window. The chance of an L1+R1 event must be equal to the L1 rate times the coincidence window time the R1 rate, and we must multiply by two to account for R1+L1 events, which are indistinguishable to the EDS. In this manner we identify the L1 coincidence window δt_1 as $5.02 \mu\text{sec}$.

We use similar fits to estimate two additional time windows: $\delta t_2, \delta t_p$ which are the coincidence windows associated with the second or third xenon layers and the propane layer, and a window that describes the chance of getting an unflagged event δt_0 . Unflagged events occur for events with certain separations on the same signal chains [4]. The process is very slightly more complicated when we fit Vp+L1 or Vp+R1 vs the L1 rate. Here we assume that the window for having an L1 event followed by a Vp event is known: the window for a Vp event followed by an L1 event is then the quadratic coefficient minus δt_1 .

The entire process was repeated using the 2 second readouts and a number of bursts from J1744-28 (96Jan27). Because the incident spectrum is quite different, the derived coincidence windows are different, particularly on the first layer. Table 1 contains all of the derived windows.

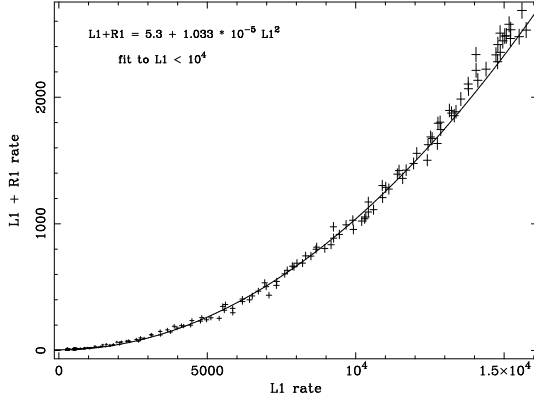


Figure 3. L1+R1 rate fit as a quadratic function of L1 rate. Both rates have been corrected for ADC deadtime. The fit is restricted to $L1 \leq 10^4$ but provides a reasonable description of the data at all observed rates.

Table 1
Coincidence timing windows

	Sco X-1	J1744-28
	μsec	
δt_0	5.0	6.5
δt_p	4.5	3.2
δt_2	9.2	9.5
δt_0	1.8	4.2

Two additional pieces of information are needed to infer incident rates from observed coincidence rates. First, the nonparalyzable deadtime associated with the analog to digital conversion is taken to be $9\mu\text{sec}$ [4]. This value is independent of pulse height, and can be used for all sources. Second, we need the ratio of source related events which interact in each layer of the detector, which is obviously dependent on the spectrum. For J1744-28 we rely on the fact that the bursts apparently have the same spectrum as the persistent emission [5], and use the persistent emission to derive the ratios L1:L2:L3:VP to be 1000:150:75:180. (The rate on R1 is assumed equal to that on L1, and similarly for the other xenon layers). For Sco X-1, we measure the relative incident ratios from the scanning data obtained relatively far from the peak and obtain 1000:67:21:440 (confirming our earlier statement that Sco X-1 has a much softer spectrum than J1744-28).

4.1. Predicting the Coincidence Rate

Our convention is that “incident rate” means the incident rate on the xenon layers. We can calculate the corresponding number of events observed in the propane layer. For a given incident rate, we calculate the incident rate on each signal chain R_j where the index j runs from 1 to 7 and corresponds to L1, R1, L2, R2, L3, R3, and VP. The observed rate of 2 lower level discriminator events, R_{2LLD} observed is given by

$$R_{2LLD} = A \sum_j \sum_{i \neq j} R_j \delta t_j R_i \quad (1)$$

where δt_j is defined as δt_1 for $j = 1, 2$, as δt_2 for $j = 3, 4, 5, 6$, and as δt_p for $j = 7$. A accounts for deadtime due to the non-paralyzable ADC process and is calculated as $r_{in}/(1 + r_{in}t_d)$. Since these are predicted rates, we have complete knowledge about the assumed incident rate r_{in} . The observed rate of unflagged events, R_{noflag} , and the observed rate of triply flagged events, R_{3LLD} , are similarly calculated:

$$R_{noflag} = A \sum_j R_j \delta t_0 R_j \quad (2)$$

$$R_{3LLD} = A \sum_j \sum_{i \neq j} \sum_{k \neq i, j} R_j \delta t_j R_i R_k \quad (3)$$

In order to predict the Remaining Count rate as recorded in the Standard 1 data, all three terms

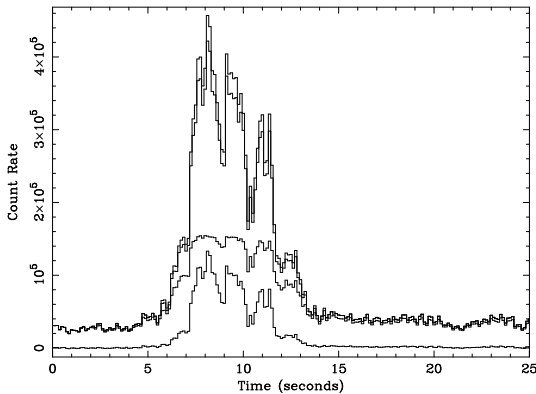


Figure 4. Good count rate, Coincident count rate, and two different estimates of the incident count rate. See text for details. The lower estimate of the corrected rate is our best estimate.

must be added (for the bursts from J1744-28, the four fold coincidence rate shows a detectable rise associated with the burst, but it is not a significant contributor to the remaining rate). In all cases, A must be evaluated considering all events (in other words, propane events always contribute to the ADC deadtime).

Figure 4 shows the same data as figure 1, along with the corrected count rate. We corrected the count rate twice, once using the coefficients derived from J1744-28 and once using the coefficients derived from Sco X-1. In both cases we assume the relative count rate distribution between the layers appropriate for J1744-28. The higher correction, which peaks at about 4.6×10^5 count/sec is associated with the coefficients for Sco X-1, while the curve that peaks near 4.2×10^5 count/sec was derived using the J1744-28 coefficients. That the two curves differ by only 10% demonstrates the expected robustness of this technique if one or the other set of coefficients is used for a different bright source such as the Soft Gamma Repeater SGR 1806-20. It is easy to see why the Sco X-1 coefficients result in a higher inferred incident rate. Since we use the coincidence rate to infer the incident rate, since the count rate on the L1 and R1 layers is the most impor-

tant contributor, and since the coincidence window derived from J1744-28 data is *longer* than that derived from the Sco X-1 data, we require a slightly lower incident rate to create the same double event rate. While 10% probably is a good estimate of the net uncertainty, we note that we have reconstructed this estimate in the presence of 70% deadtime by traditional definitions! Our estimate is similar to an independent estimate [6] which derives relationships between the various coincidence rates and the good event rate without a detailed accounting for the different coincidence windows on different layers. While that model produces a similar result, and is therefore of equal phenomenological validity, they derive the value of the ADC deadtime, and consistently get a value which is larger than the measured $9\mu\text{sec}$.

5. BURST HISTORY OF J1744-28

Finally we apply the same deadtime correction discussed above to the data base of J1744-28 observations. RXTE has observed J1744-28 regularly through out the first two years of the mission ([5] [8]). Figure 5 shows the persistent flux, the peak flux in each burst, and the burst fluences. We have not included any bursts from May or June 1996; bursts at this time are either Type I X-ray bursts from another source within the field of view [7] or much fainter and more frequent bursts which are part of a different “rumbly” phenomenology [8]. The bright bursts occur only during the periods when the persistent flux is quite bright (above ~ 1000 count/sec). However, we have observed bursts over a range of persistent intensities that span one and a half orders of magnitude, and the striking feature of fig 5 is that the ratio of peak flux to persistent flux, and the ratio of burst fluence to persistent flux, remain relatively constant.

Throughout the periods of bright bursting emission, the persistent emission can be adequately described by a hard power law modified by galactic absorption and a high energy exponential cutoff. (There is also evidence for an Iron line but this does not have a large effect on the derived flux). This simple model provides the same estimated flux as the continuous model described

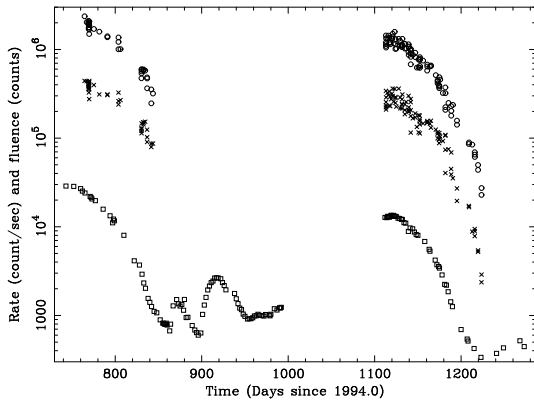


Figure 5. Persistent flux (squares), peak burst flux (crosses), and burst fluence (circles) for burst observed during observations of J1744-28. Several bursts defy the general trend; these are largely Type I bursts from other sources in the field of view ([8]).

by [9]. We find that the 2-10 keV flux is $1.81 \times 10^{-12} \text{erg sec}^{-1} \text{cm}^{-2}$ per count/sec (counts/sec measured in all PCA channels); the 2-40 keV flux is $4.95 \times 10^{-12} \text{erg sec}^{-1} \text{cm}^{-2}$ per count/sec; the 2-100 keV flux is $5.40 \times 10^{-12} \text{erg sec}^{-1} \text{cm}^{-2}$ per count/sec. Taking the highest estimated peak fluxes for bursts in the first outburst, with peak rates of 4.4×10^5 count/sec, we derive a peak flux of $2.4 \times 10^{-6} \text{erg sec}^{-1} \text{cm}^{-2}$. The corresponding peak luminosity is $1.8 \times 10^{40} d_8^2 \text{erg sec}^{-1}$ where d_8 is the distance to J1744-28 normalized to 8 kpc. This is about 100 times the Eddington luminosity given typical values for a neutron star mass and radius. Given the nearly constant ratio of burst fluence to persistent flux, we conclude that the ratio α of persistent flux to time averaged burst flux must be approximately constant (to the extent that the average interval between bursts is constant). We previously reported that $\alpha \sim 34$ in January 1997 [10] and take this as a representative value for both major outbursts.

None of the above conclusions could be reliably drawn from the good counting rate alone, but require the extra information contained in the co-

incidence rate. The most important conclusion may therefore be our recommendation to future users of the RXTE satellite who may be observing extremely bright sources: use modes which include some coincidence information at the highest timescales of interest. On a practical level, extremely bright sources may be thought of as those which produce $\geq 15,000$ count/sec/PCU with associated deadtimes of $\geq 15\%$. An example of the value of this approach for observations of Sco X-1 is given in [11].

Comparisons to the Crab nebula are often ambiguous due to the different spectral shapes. However, limiting the comparison to total count rate (13,000 count/sec for the Crab), we find that the bursts reached 34 Crab. Put another way, we can recast our subtitle (using “!” for “i”): *A grand one man band with major lighting: stops at 17 $\frac{4}{\text{two}}$ Crab !!*

We thank the organizing committee and all participants for a stimulating workshop, and Prof. Bignami for challenging us to present our result anagrammatically.

REFERENCES

1. C. Kouveliotou et al. 1996, Nature, 379, 799.
2. http://heasarc.gsfc.nasa.gov/RPS/XTE/pca_valid_configs.txt
3. W. Zhang et al. 1993, Proc. SPIE 2006, p. 324.
4. K. Jahoda et al., 1996 Proc. SPIE 2808, p. 59.
5. A. B. Giles et al. 1996, Ap. J. Lett., 469, L25.
6. D. Fox et al., 1998, in preparation.
7. T. E. Strohmayer et al. 1997, Ap. J., 486, 355.
8. M. J. Stark et al. 1998, in preparation; also Stark et al., astro-ph/9712154.
9. W. Heindl 1998, this volume.
10. T. E. Strohmayer et al. 1997, Proc. 4th Compton Symposium, AIP CP410, p. 692.
11. M. van der Klis et al. 1996, Ap. J. Lett., 469, L1.